Water diffusion in brain cortex closely tracks underlying neuronal activity

Tomokazu Tsurugizawa, Luisa Ciobanu, and Denis Le Bihan[1]

NeuroSpin, Bât 145, Commissariat à l'Energie Atomique-Saclay Center, 91191 Gif-sur-Yvette, France

Edited by Pierre J. Magistretti, Ecole Polytechnique Fédérale de Lausanne, Lausanne, Switzerland, and accepted by the Editorial Board June 6, 2013 (received for review February 18, 2013)

Neuronal activity results in a local increase in blood flow. This concept serves as the basis for functional MRI. Still, this approach remains indirect and may fail in situations interfering with the neurovascular coupling mechanisms (drugs, anesthesia). Here we establish that water molecular diffusion is directly modulated by underlying neuronal activity using a rat forepaw stimulation model under different conditions of neuronal stimulation and neurovascular coupling. Under nitroprusside infusion, a neurovascular-coupling inhibitor, the diffusion response and local field potentials were maintained, whereas the hemodynamic response was abolished. As diffusion MRI reflects interactions of water molecules with obstacles (e.g., cell membranes), the observed changes point to a dynamic modulation of the neural tissue structure upon activation, which remains to be investigated. These findings represent a significant shift in concept from the current electrochemical and neurovascular coupling principles used for brain imaging, and open unique avenues to investigate mechanisms underlying brain function.

The noninvasive monitoring and imaging of neuronal activity in vivo in the intact brain is of primordial importance to understand mechanisms underlying brain function. Most approaches, so far, have relied on the neurovascular coupling principle (1): Neuronal activity results in a local increase in metabolism and blood flow. This concept has been extremely fecund, leading to the current modality for functional MRI (fMRI) (blood oxygenation level-dependent (BOLD) method (2), which relies on variations of the blood deoxyhemoglobin content in the vasculature induced by the changes in blood flow. Still, the mechanisms of the neurovascular coupling are not yet fully understood (3, 4). Furthermore, this fMRI approach presents some limitations, as its link with neuronal activity remains indirect and BOLD fMRI responses may be significantly altered or even suppressed in situations when the neurovascular coupling mechanisms are compromised (drugs and anesthesia) (5, 6). Besides the neurovascular and electrochemical (action potential and neurotransmission) coupling principles, which have prevailed in neuroscience and have been investigated in several ways (7, 8) as candidates for fMRI, there might be other elementary mechanisms intimately linked to neuronal activity, which may have been overlooked. Dynamic changes in the tridimensional neuronal tissue microstructure induced by neuronal activation have been observed for several decades in individual cells (9), brain slices (10), and in vivo, mainly using various types of optical measurements, and there is now growing evidence that neuronal swelling occurs during activation. It has been well established that MRI can be made sensitive to tissue microstructure through the measurement of water molecular diffusion (11) and preliminary attempts have been made that suggest that diffusion MRI (DfMRI) could have the potential to monitor such activation-induced tissue changes (12–15), although residual effects from the hemodynamic changes underlying the BOLD mechanism could interfere with the diffusion measurements (16, 17).

Here we establish that local water diffusion is, indeed, directly modulated by underlying neuronal activity using a rat forepaw stimulation model under different conditions of neuronal stimulation and neurovascular coupling. The results show that the diffusion response is not of vascular origin and is closely linked to the neuronal response patterns. The observed diffusion changes point to a dynamic modulation of the neural tissue structure upon activation.

Results

Comparison of DfMRI, BOLD, and Local Field Potential Response Time Courses. We first calculated activation maps for gradient echo (GE)-BOLD, spin echo (SE)-BOLD, and DfMRI signals during a 7-Hz forepaw electrical stimulation paradigm under 1.5% isoflurane anesthesia using the raw local field potential (ΣLFP) as the temporal template. An activation spot was found for DfMRI and SE-BOLD at the tip of the recording electrode (Fig. 1). In contrast, the GE-BOLD activation spots extended largely outside of this location (remote vascular effects or false positive activation).

We then compared the temporal pattern of signal responses in a small region of interest (ROI) within the somatosensory cortex located at the tip of the recording electrode (Fig. 1*A*). As shown in Fig. 2, the peak amplitude of DfMRI response was slightly greater than the BOLD responses. The GE- and SE-BOLD signals increased at the beginning of the stimulation period and remained high, slowly decreasing over time. The DfMRI signal peaked earlier than the BOLD signals (3.3 ± 0.6 s, 3.3 ± 0.6 s, and 1.8 ± 0.6 s in GE-BOLD, SE-BOLD, and DfMRI, respectively), consistent with previous findings in human visual cortex, although the DfMRI advance over BOLD was smaller than reported earlier (13). The ΣLFPs peak apparently occurred slightly earlier than the DfMRI signal (0.29 ± 0.87 s), but the time difference remained within limits of the lower temporal resolution of MRI. Strikingly, the DfMRI response decreased immediately after the peak in a very similar way as the LFPs, much earlier than the BOLD responses. Overall, although some adaptation and habituation effects could be seen for all signals (decrease of the response amplitude across blocks after the first stimulus and also within blocks) (18, 19), the shape of the DfMRI response time course matched very closely that of the LFPs, whereas the BOLD response time courses showed a marked time lag in their decay, reflecting their intrinsic convolution with the slow hemodynamic responses.

Modulation of Neurovascular Coupling with Nitroprusside. To disrupt the hemodynamic response associated with the electrical stimulation, we used nitroprusside, which is known to interfere with or even suppress the neurovascular coupling through vasodilation (5).

Author contributions: T.T. and D.L.B. designed research; T.T. and L.C. performed research; T.T. and D.L.B. analyzed data; and T.T., L.C., and D.L.B. wrote the paper.

The authors declare no conflict of interest.

This article is a PNAS Direct Submission. P.J.M. is a guest editor invited by the Editorial Board.

[1]To whom correspondence should be addressed. E-mail: denis.lebihan@gmail.com.

This article contains supporting information online at www.pnas.org/lookup/suppl/doi:10.1073/pnas.1303178110/-/DCSupplemental.

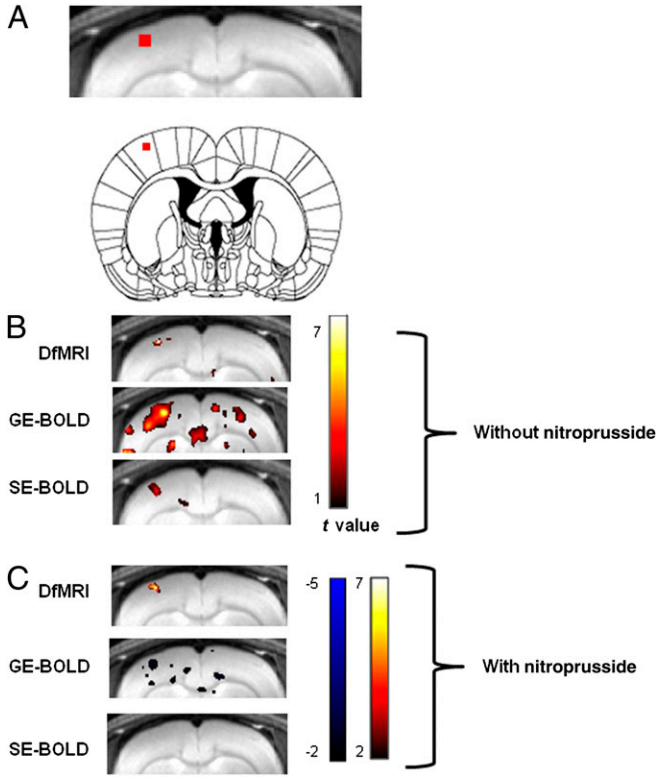

Fig. 1. (*A*) Location of the electrophysiologically recorded area in the somatosensory cortex. (*B*) Group activation maps (*t* contrast) for the BOLD and diffusion MRI signals obtained from a 7-Hz forepaw electrical stimulation paradigm under 1.5% isoflurane anesthesia by using as a regressor the ΣLFP signal. (*C*) Group activation maps obtained after nitroprusside infusion. Color bars, *t* values.

As expected, under i.v. administration of nitroprusside, blood pressure significantly decreased from 72 ± 6 mmHg to 34 ± 8 mmHg; however, there was no significant change in pO_2, pCO_2, and pH levels of the arterial blood during electrical stimulation with or without nitroprusside (pO_2/pCO_2: 46.4 ± 3.9/95.2 ± 14.3 mmHg without nitroprusside, 53.5 ± 2.3/99.0 ± 9.0 mmHg with nitroprusside), in accordance with a previous report (20).

The activation maps obtained at 7-Hz electrical stimulation under 1.5% isoflurane anesthesia show that the DfMRI response location and amplitude were maintained with nitroprusside, whereas the SE-BOLD activation spots disappeared (Fig. 1*C*). Some negative GE-BOLD spots were visible (oxygen consumption). Indeed, the GE-BOLD, SE-BOLD, and low b-value DfMRI responses were abolished or slightly negative (GE-BOLD: −0.31 ± 0.06%; SE-BOLD: −0.12 ± 0.05%; b = 250 s/mm^2: −0.08 ± 0.06%) (Fig. 3 *A* and *B*), in agreement with a previous study (5). In contrast, the DfMRI response was maintained, although the overall peak was amputated by a similar amount (−0.34% on average). Overall, the DfMRI response peak increased with the b value in a similar way in the without and under nitroprusside infusion conditions (b = 1,000 s/mm^2: 0.63 ± 0.11%; b = 1,800 s/mm^2: 1.04 ± 0.12%; b = 2,600 s/mm^2: 2.26 ± 0.44% without nitroprusside, and b = 1,000 s/mm^2: 0.32 ± 0.18%; b = 1,800 s/mm^2: 0.70 ± 0.24%; b = 2,600 s/mm^2: 1.7 ± 1.0% with nitroprusside) (Fig. 3*B*). The peak value of the ∑LFP at 7-Hz stimulation was not affected by nitroprusside, in agreement with a previous study (20) (Fig. 3*C*). The peak change in the water apparent diffusion coefficient (ADC) induced by the stimulus was around −6%, but not significantly different without and under nitroprusside (−5.98 ± 1.64 and −6.75 ± 3.10%, respectively) (Fig. 3*D*).

Hyperoxia Challenge. To further establish the nonvascular origin of the diffusion component of the DfMRI response, we submitted the animals to a hyperoxia challenge, which mimics a BOLD response in the absence of neuronal activation (without electrical stimulation). Indeed, no LFP-evoked response could be observed (Fig. 4*A*). In contrast to the neuronal stimulation condition, under hyperoxia, the DfMRI signal change was two to three times smaller than those of the GE- and SE-BOLD signals (GE-BOLD, 5.3 ± 1.4%; SE-BOLD, 4.0 ± 0.9%; b = 250, 2.7 ± 0.8%; b = 1,800, 1.7 ± 0.4%; b = 2,600, 1.5 ± 0.6%) (Fig. 4 *A* and *B*). The amplitude responses for the b = 1,800 s/mm^2 and b = 2,600 s/mm^2 DfMRI signals were not significantly different and there was no significant change in ADC induced by hyperoxia (−0.7 ± 0.9%) (Fig. 4*C*). After 3 min from the replacement of air, the DfMRI response decreased to the baseline, whereas the BOLD signal remained significantly higher than baseline level (GE-BOLD, 2.2 ± 0.4%; SE-BOLD, 1.2 ± 0.6%). The saturated O_2 level in the arterial blood significantly increased from 89 ± 5 mmHg to 501 ± 89 mmHg under the hyperoxic condition, returning to 86 ± 3 mmHg under air.

Modulation of Neuronal Response by Stimulus Frequency and Amplitude. Next we investigated the frequency dependence of BOLD and DfMRI responses to electrical stimulation under 1.5% isoflurane anesthesia as the neural adaptation is known to depend upon the stimulation frequency (21). Four frequencies (3, 7, 10, and 13 Hz) were used, whereas the other parameters of

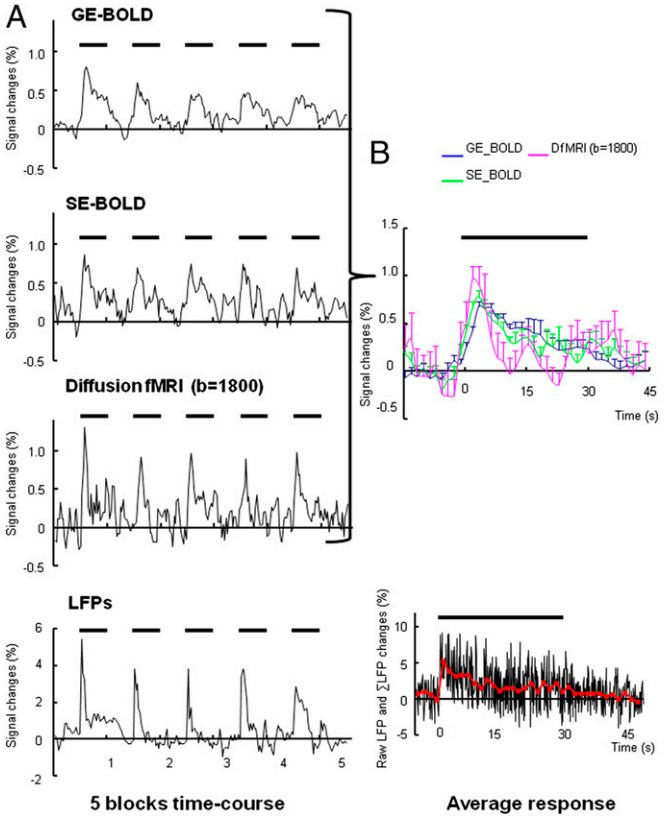

Fig. 2. (*A*) Five-block time courses for BOLD (SE and GE) and DfMRI responses, and LFPs (averaged over animals) recorded from a 7-Hz forepaw electrical stimulation paradigm under 1.5% isoflurane anesthesia. (*B*) Corresponding averaged responses (over animals and blocks) for the BOLD (SE and GE) and DfMRI signal. Data were expressed as mean ± SEM.

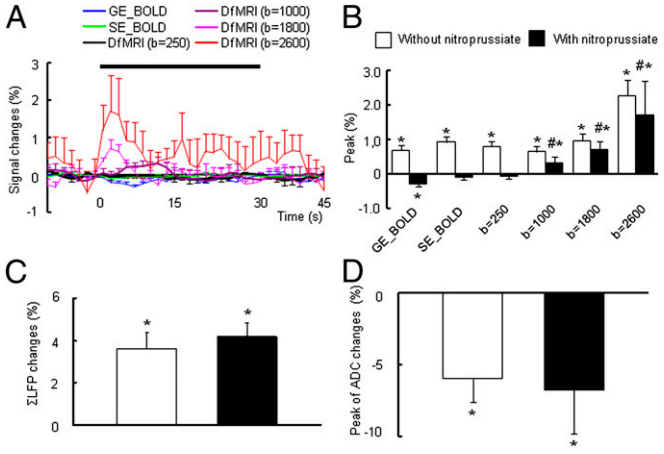

Fig. 3. (*A*) Time course of BOLD (GE and SE) and DfMRI (b = 250, 1,000, 1,800, and 2,600) response to 7-Hz stimulation with the nitroprusside administration under 1.5% isoflurane level. (*B*) Peak value of BOLD and DfMRI responses, (*C*) ∑LFP, and (*D*) ADC changes with and without nitroprusside under 1.5% isoflurane levels; $^{*}P < 0.05$ compared with basal; $^{\#}P < 0.05$ compared with GE and SE. Statistical comparison between BOLD and DfMRI (all b value) was done using ANOVA and post hoc Tukey–Kramer test for group comparisons. The statistical comparison with the basal level was done using paired *t* test. Data were expressed as mean ± SEM.

the electrical stimulation were fixed. The peak value of the DfMRI response was slightly higher than the BOLD responses in the range of 3–13 Hz (significantly higher for 3 and 10 Hz) (Fig. 5*A*). The peak value of ΣLFP was similar across all frequencies (Fig. 5*B*). Averaged time courses for all fMRI signals and LFPs are shown in Fig. S1.

The time-to-peak in DfMRI was shorter than SE- and GE-BOLD at all frequencies, except for the SE-BOLD response, which was found similar to DfMRI at 10 Hz (Fig. 5*C*). The time-to-peak of ΣLFP remained significantly shorter than both BOLD and DfMRI signals at all frequencies, but the time difference between DfMRI and ΣLFP time-to-peak values remained within the temporal resolution limit of DfMRI. The DfMRI signal decreased significantly faster than BOLD at 7–13 Hz, resulting in narrower full widths at half maximums (FWHMs) (6.3 ± 0.7 s, 7.8 ± 1.7 s, and 6.3 ± 0.3 s at 7, 10, and 13 Hz, respectively) than the GE-BOLD FWHMs (19.8 ± 2.0 s, 15.3 ± 1.4 s, and 15.3 ± 3.6 s at 7, 10, and 13 Hz, respectively) and SE-BOLD FWHMs (12.3 ± 1.4 s, 15.3 ± 1.4 s, and 9.3 ± 3.6 s at 7, 10, and 13 Hz, respectively) (Fig. 5*D*). The FWHMs of the DfMRI response, BOLD response, and ΣLFP at 3 Hz were significantly larger than those at 7–13 Hz. The FWHM of ΣLFP was narrower than those of GE- and SE-BOLD DfMRI signals at 7–13 Hz, but was similar to DfMRI at all frequencies (13.8 ± 4.3 s, 7.8 ± 1.0 s, 4.8 ± 1.3 s, and 4.8 ± 1.6 s for 3, 7, 10, and 13 Hz, respectively).

The 7-Hz stimulation was also performed at a higher stimulus level (7 mA instead of 2 mA) to check for possible correlation of the signal responses with stimulus strength. Although a global trend in the amplitude response (increasing from 2 to 7 mA) could be observed, the change was not significant. No change in FWHM or time-to-peak was visible, except perhaps for the SE-BOLD time-to-peak, which was shorter at 2 mA. The time-to-peak and FWHM of DfMRI and ΣLFP were still narrower than GE-BOLD at 7 mA (Fig. S2).

Modulation of Neuronal Response and Neurovascular Coupling by Isoflurane Level. Isoflurane is an anesthetic agent known to disrupt neurovascular coupling (22), depending on dosage, as well to suppress the neural activity in cerebral cortices (23–25). Because isoflurane is not only a vasodilator but also a modulator of neurovascular coupling, it can disturb the behavior of the hemodynamic response nonlinearly. The BOLD and DfMRI responses at 7-Hz electrical stimulation were dependent on isoflurane level. The peak value of BOLD signals increased from 1.0% to 1.5% isoflurane level and remained stable between 1.5% and 2% (GE-BOLD: 0.53 ± 0.05%, 0.68 ± 0.15%, and 0.62 ± 0.09%; SE-BOLD: 0.58 ± 0.11%, 0.92 ± 0.15%, and 0.77 ± 0.06% for 1.0, 1.5, and 2.0%, respectively) (Fig. 6*A*). In contrast, the peak of DfMRI responses was significantly lower at 2.0% isoflurane (0.42 ± 0.12%) compared with those observed at 1.0% and 1.5% isoflurane levels (1.10 ± 0.16% and 0.96 ± 0.19%, respectively). The peak of ΣLFP under 2.0% isoflurane was also significantly lower than with 1.0% and 1.5% isoflurane (4.02 ± 0.42%, 3.64 ± 0.78%, 2.06 ± 0.74% for 1.0, 1.5, and 2.0%, respectively), matching the DfMRI response pattern (Fig. 6*B*). The averaged time courses for all MRI signals are shown in Fig. S3.

The time-to-peak differences observed at 7 Hz under 1.5% isoflurane for SE-BOLD, DfMRI, and ΣLFP were generally not affected by the dose of the isoflurane, but the GE-BOLD time-to-peak tends to be longer than SE-BOLD, although not significantly, at 1.0% and 2.0% isoflurane levels (Fig. 6*C*). The FWHMs of the ΣLFP and the DfMRI responses were similar and narrower than for GE-BOLD and SE-BOLD under all isoflurane levels (Fig. 6*D*).

Discussion

The series of results we obtained under different conditions of neuronal stimulation and neurovascular coupling show that the diffusion response is not of vascular origin and is closely linked to the neuronal response. The decrease of neural activation after the first forepaw stimulation can been ascribed to neuronal habituation effects (18, 19). This effect across activation blocks was observed in both diffusion MRI and BOLD signals (Fig. 2). However, within blocks, the LFPs showed a sharp decrease after the stimulation onset, a neuronal adaptation effect (21, 26), which the DfMRI signal was precisely able to pick up. On the

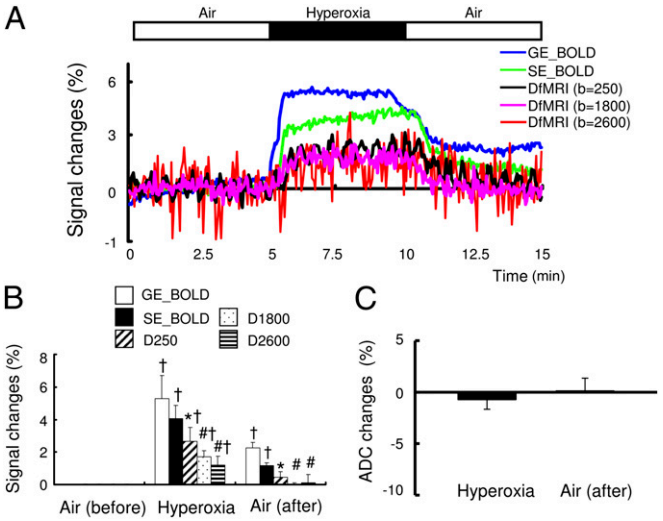

Fig. 4. (*A*) Time course of BOLD (GE and SE), diffusion-weighted MRI (b = 250, 1,800, and 2,600) and ΣLFPs responses with hyperoxia condition under 1.5% anesthesia. (*B*) Peak value of BOLD and DfMRI responses and (*C*) ΣLFP changes. $^{*}P < 0.05$ compared with GE-BOLD; $^{\#}P < 0.05$ compared with GE- and SE-BOLD; $^{\dagger}P < 0.05$ compared with basal. Statistical comparison between BOLD and DfMRI (all b value) was done using ANOVA and post hoc Tukey–Kramer test for group comparisons. The statistical comparison with the basal level was done using paired *t* test. Data were expressed as mean ± SEM.

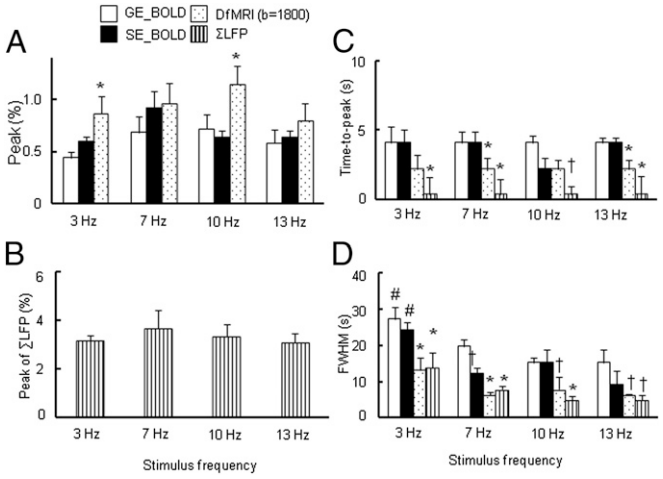

Fig. 5. (*A*) Peak value of BOLD, DfMRI (b = 1,800 s/mm^2) responses and (*B*) ΣLFP, (*C*) time-to-peak of BOLD and DfMRI, (*D*) FWHM of BOLD and DfMRI responses by four stimulation frequencies (3, 7, 10, and 13 Hz) under 1.5% isoflurane anesthesia; $^*P < 0.05$ compared with GE-BOLD and SE-BOLD in each frequency; $^{\dagger}P < 0.05$ compared with GE-BOLD in each frequency; $^{\#}P < 0.05$ compared with 7 Hz in each method. Statistical comparison between BOLD and DfMRI was done using ANOVA and post hoc Tukey–Kramer test for group comparisons. Data were expressed as mean ± SEM.

contrary, the hemodynamic response did not show this neural adaptation effect as clearly, the response lagging after its onset, in agreement with previous studies (26, 27). Whereas the mechanisms for this neural adaptation are not fully understood, it is known that isoflurane may play an active role (28). Although a correlation of the BOLD response with LFPs has been established (3), its indirect link with neuronal events through the slow neurovascular coupling mechanism hampers fast variations in neuronal activity from being visible. To the contrary, the sharp DfMRI response can apparently pick up such fast events, suggesting that the DfMRI response is either directly linked to neuronal events or linked through a fast coupling mechanism.

Strikingly, the BOLD responses were completely quenched with nitroprusside, as shown previously (5, 20), whereas the DfMRI responses were only slightly suppressed and the neuronal response remained intact, as shown with the LFP recording. The slight negative response observed with the GE-BOLD sequence reflects the local increase in blood deoxyhemoglobin content due to oxygen consumption revealed by the suppression of the blood flow increase with nitroprusside (5). Those patterns were also seen in the ventral posterolateral nucleus (VPL) of the thalamus (Fig. S4).

Indeed, the DfMRI response is the sum of a genuine diffusion component and a residual relaxivity (T2′) component (29):

$$S/So = \exp(TE/T2')\exp(-b\ ADC), \qquad [1]$$

where S/So is the signal attenuation, TE the echo time, T2′ the relaxation time, and ADC the apparent diffusion coefficient. The link of the diffusion component with neuronal activation has been suggested in the past (12, 13) and demonstrated in isolated brain slices (15).

Several groups have argued that the relaxivity component, which results from local variations in local susceptibility induced by variations in vascular deoxyhemoglobin content (at the origin of the BOLD response) may completely obscure the diffusion component in vivo (16, 17, 29). Although this hypothesis is verified with b = 250 s/mm^2, our results clearly establish this is not the case when the DfMRI signal is acquired at a high level of diffusion weighting (high b values). It is expected that the contribution of the diffusion component increases with amount of diffusion weighting (b value) (13). This is exactly what we have observed, whereas the amount of signal amputation under nitroprusside did not differ significantly across b values from 1,000 to 2,600 s/mm^2. Effects of local variations in vessel size (blood volume), which could modulate the overall MRI signal (30) and perhaps water diffusion in the tissue, are also ruled out as blood volume variations are abolished with nitroprusside. In any case, such vasculature-related components (in addition to T2′) would not share the time course of the diffusion components if they result from different mechanisms. The small DfMRI response observed during hyperoxia, independent of the b value, is well explained by the relaxivity component, whereas the diffusion component is absent in this condition, given there is no neuronal activation.

Our results for the DfMRI response and LFPs under various isoflurane levels are in agreement with those of a previous study (26), which showed that neural activation in the primary somatosensory cortex was decreased, whereas the BOLD signal was not changed or even slightly increased at a high dose of isoflurane under 7-Hz electrical stimulation. These results, together with the modulation of the neuronal response by stimulus frequency, also indicate that the DfMRI response and the ADC (Fig. S1*E*) more directly reflect neural activity than the BOLD response. The effects of isoflurane on neural tissue and hemodynamics are complex. Isoflurane is an anesthetic agent known to disrupt neurovascular coupling (22, 26), depending on dosage, as well as to suppress the neural activity in cerebral cortices (23–25). Because isoflurane is not only a vasodilator, but also a modulator of neurovascular coupling, it can disturb the behavior of the hemodynamic response nonlinearly (31). The mechanisms of the isoflurane-induced disturbance of the neurovascular coupling are not yet fully understood. Vasodilators such as isoflurane and halothane have direct effects on cerebral vascular smooth muscle (22). Isoflurane also suppresses the release of neurotransmitters from the synaptosomes of cortical neurons (32–34) and reduces neural activity in the cerebral cortex (23, 24). Using calcium imaging in the activated visual cortex of the ferret, Schummers et al. have shown that isoflurane modulates the neurovascular coupling level by decreasing astrocyte activity, while preserving neuron activity (35). In our study, however, the DfMRI and LFP peaks decreased at 2.0% isoflurane, whereas the BOLD response remained high, perhaps reflecting the nonlinear relationship between the neural activity and the hemodynamic response (31).

In summary, altogether these results demonstrate that the DfMRI response contents a component which is not of vascular origin and is closely linked to the neuronal response patterns (amplitude modulation and time course, including adaptation effects). This component is better seen at a high degree (high b value) of diffusion weighting. As diffusion MRI exquisitely reflects how molecular water displacements in tissues are affected by obstacles, in particular cell membranes, the observed diffusion changes point to a dynamic modulation of the neural tissue structure upon activation. The direct observation of such functional structural changes represents a significant shift in concept from the neurovascular coupling principle. Beside established mechanisms, such as electrochemical coupling, one may envision other kinds of couplings within neural tissues that could have been overlooked, such as a neuromechanical coupling linking the shape of cells or cell elements (neurons, dendritic spines, and possibly astrocytes) with their activation status. The contribution of the astrocyte to the BOLD response has been documented, as the astrocyte seems to play a key role in neurovascular coupling, which is at the origin of the BOLD response (27, 36, 37). As for the DfMRI response, if cell swelling is the associated mechanism, we cannot determine at this stage which cell type or element within the neuropile contributes the most. Most existing literature has focused on dendritic spine twitching and neuronal swelling (38), but there are a few reports

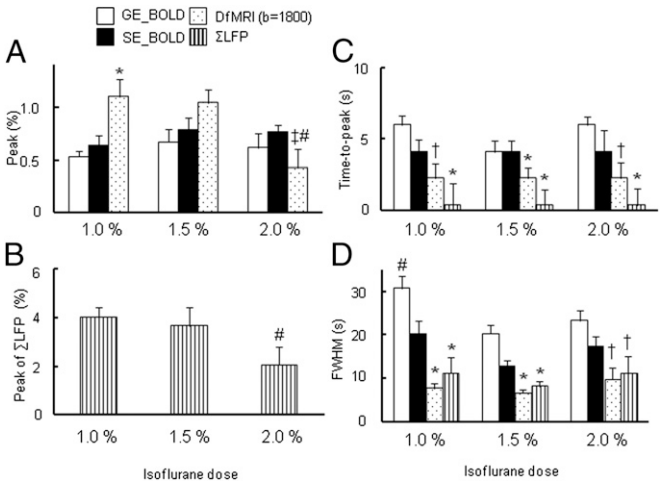

Fig. 6. (*A*) Peak value of BOLD, DfMRI (b = 1,800 s/mm^2) responses and (*B*) ΣLFP, (*C*) time-to-peak of BOLD and DfMRI by 7-Hz stimulation under 1.0%, 1.5%, and 2.0% isoflurane and (*D*) FWHM of BOLD and DfMRI responses; $^*P < 0.05$ compared with GE-BOLD and SE-BOLD in each dose; $^{\dagger}P < 0.05$ compared with GE-BOLD in each dose; $^{\ddagger}P < 0.05$ compared with SE-BOLD; $^{\#}P < 0.05$ compared with other dose in each method. Statistical comparison was done using ANOVA and post hoc Tukey–Kramer test for group comparisons. Data were expressed as mean ± SEM.

on glial cell swelling (39). In any case, studies based on optical recordings are indeed sensitive to the reduction of the extracellular space associated with cell swelling, and not specific to any particular cell population. Using calcium imaging, however, Schummers et al. (35) have shown that isoflurane may decrease or even abolish specifically the astrocyte response (and associated hemodynamic response), whereas the neuronal response remains almost intact. The discrepancy we have observed between the BOLD and DfMRI behaviors under different levels of anesthesia might reflect this differential cell-type sensivity to isoflurane, pointing out that the DfMRI response may be more neuronal than glial. Although further investigation is necessary to clarify the mechanisms responsible for the observed diffusion response (biophysical link between cell swelling and ADC decrease) (40) and its precise relationship with neuronal activity (excitatory and inhibitory spike activity, local action potentials), water molecular diffusion already appears as a biomarker of neuronal activation and DfMRI as a very promising tool to carry out fMRI studies in conditions where neurovascular coupling could be compromised and the hemodynamic response altered, as a result of anesthesia, the presence of interfering drugs, pathology, or perhaps even in some physiological conditions.

Materials and Methods

Animal Preparation. BOLD, DfMRI, and LFP measurements were performed on 90 male Wistar rats (180–250 g, Janvier Labs, Saint Berthevin, France). The rats were housed two per cage under controlled light (7:00–19:00) conditions and were given free access to water and food. All animal procedures in the present study were approved by the Comité d'Ethique en Expérimentation Animale, Commissariat à l'Energie Atomique et aux énergies alternatives, Direction des Sciences du Vivant (Fontenay-aux-Roses, France). The number of animals assigned to each condition was as follows: 1% (vol/vol) isoflurane anesthesia $n = 8$ for 7-Hz forepaw stimulation; 1.5% (vol/vol) isoflurane anesthesia $n = 7$, 13, 10, and 9 for 3-, 7-, 10-, and 13-Hz forepaw stimulation, respectively; 2% (vol/vol) isoflurane anesthesia $n = 10$ for 7-Hz stimuli; nitroprusside $n = 14$; hyperoxia (100% O_2) $n = 11$; and electrophysiology $n = 8$.

The animals were initially anesthetized with isoflurane (3% for induction and 1.0–2.0% for maintenance) in air (20% O_2). For all MR experiments, the animals were intubated and mechanically ventilated (MRI ventilator; CWE, Inc.). The respiration rate and body temperature were monitored throughout the experiment. Body temperature was maintained at 36 °C using an MR-compatible, feedback-controlled air heating system (model 1025; SA Instruments). In the electrophysiological study, the animals anesthetized with 2.5% isoflurane were placed in a stereotaxic frame (David Kopf Instruments), and a hole, centered at 3.7 ± 0.2 mm lateral and 0.7 mm rostral from the Bregma, was drilled on the left side of the skull. After the surgery, the isoflurane concentration was changed to 1.5%.

Electrical Stimulation. To perform the electrical forepaw stimulation, two needle electrodes (26 gauge) were inserted under the skin in digits 2 and 4 of the right forepaw. Electrical pulse stimulation was given with a constant current bipolar isolated pulse stimulator (model 2100; A-M Systems), triggered by a transistor-transistor logic pulse from the Bruker imaging system. The rectangle pulses with 3-ms duration, 2-mA current, and four distinct frequencies (3 Hz, 333-ms interval; 7 Hz, 143-ms interval; 10 Hz, 100-ms interval; or 13 Hz, 75-ms interval) were applied five times for 30 s, separated by a 30-s or 60-s rest interval (Fig. 1*A*). This relatively long stimulation period was chosen in order to see neuronal adaptation effects (21, 27). Stimulation at 7 Hz was also performed in seven rats at 7 mA to investigate possible effects of stimulus strength.

Hyperoxia. For the hyperoxia condition (with no stimulation), 5 min after the beginning of the acquisition, air containing 20% oxygen was replaced by 100% oxygen for 5 min, before switching again to air containing 30% oxygen accounting for a total acquisition time of 15 min.

Nitroprusside Challenges. To suppress the neurovascular component, sodium nitroprusside (Sigma-Aldrich) was continuously infused into the tail vein at the rate of 0.01 mg/min per 200 g body weight, while the right forepaw was stimulated as described above. Blood pressure (model 1025; SA Instruments), blood O_2 saturation, CO_2 saturation, and pH levels (ABL5 radiometer) were monitored.

Electrophysiology. The electrophysiological experiments were performed outside the magnet (21), as it would be technically challenging to record usable signals in the MRI system environment, under heavy radiofrequency and gradient pulsing. Besides, simultaneous recording of BOLD and diffusion fMRI signals cannot be achieved by principle, as only one MRI signal can be acquired at a given time. To compare the neural activity with MRI signal changes, we recorded LFP in layer 2–3 of the somatosensory cortex. Layer 2–3 is rich in pyramidal dendrites (whereas pyramidal cell bodies lie mainly in layer 4–5), and light transmittal studies (which is sensitive to cell swelling) have shown that responses to electrical stimulation were larger and faster there (38). LFPs have been shown to match the BOLD response better than multiunit responses (3). LFPs in the somatosensory cortex were continuously recorded with a single tungsten microelectrode. The electrode tip (<1.0 MΩ, a 1-μm tip and 0.127-mm shaft diameter; Alpha Omega Engineering) was positioned at a depth of about 0.5 mm from the cortical surface. LFP signal were acquired at 1-kHz sampling rate using dedicated data acquisition software (Cheetah; Neuralynx). The reference electrode was positioned on the scalp. To compare the LFP change and MRI signal change, we used identical forepaw stimulation parameters. LFPs were recorded twice each time and then averaged. The amplitude of evoked LFP was calculated as the difference between the positive and negative peaks. To compensate for the low time resolution of MRI (1.5 s) an average LFP response (ΣLFP) was then calculated by summing LFP amplitudes within intervals of 1.5 s.

MRI Procedure. MRI experiments were performed on a horizontal bore, 7T MRI scanner (PharmaScan; Bruker) equipped with a gradient system allowing a maximum gradient strength of 760 mT/m. A dedicated surface coil (30-mm diameter) was used for transmission and reception. We acquired GE-BOLD fMRI data using a T2*-weighted echo planar imaging (EPI) sequence with the following parameters: repetition time (TR) = 1,500 ms, echo time (TE) = 20 ms, flip angle = 35°, field of view (FOV) = 32 mm × 32 mm, acquisition matrix = 100 × 100, slice thickness = 1.2 mm, slice gap = 0.2 mm, slice number = 3. First, using anatomical images on three orthogonal directions, we determined the position of three slices between +2.0 and −2.5 mm from the Bregma. DfMRI images were acquired using a diffusion-sensitized double SE EPI sequence (TE/TR = 38.9/1,500 ms, b = 250; 1,000; 1,800 s/mm^2). All other parameters were identical to those for BOLD fMRI. SE-BOLD fMRI data were acquired using the diffusion-sensitized double SE EPI sequence (TE/TR = 38.9/1,500 ms) with b = 10 s/mm^2. For the highest b value (2,600 s/mm^2), we adjusted TE (TE = 28 ms), FOV (20 × 20 mm), and matrix size (64 × 64) to maximize the signal:noise ratio. The acquisition was repeated three times for b = 250 and five times for b = 1,000, 1,800, and 2,600 to compensate for lower signal:noise ratios. Signals for each b value were averaged after the experiment.

After the fMRI acquisition, structural images were obtained by multislice rapid acquisition with a relaxation enhancement (RARE) sequence using the following parameters: TR= 2,500 ms, effective TE = 60 ms, RARE factor = 8, acquisition matrix = 128 × 128, four averages.

Data Analysis. We used SPM8 software (Wellcome Trust Centre for Neuroimaging) for data preprocessing, including slice realignment, coregistration to structural images, and spatial normalization of functional data. Before preprocessing, we obtained template images coregistered to the Paxinos and Watson rat brain atlases (41). Image sets containing motion artifacts or head movement were discarded. After the spatial correlation, data were denoised using FSL MELODIC [Functional MRI of the Brain (FMRIB) Software Library].

Activation maps were calculated using SPM8 software using as regressors the ∑LFP response. SPM8 beta maps were first calculated from a fixed effect analysis and then entered into a random effect analysis by using a one-sample *t* test analysis. Activation maps were plotted at a threshold of $P < 0.001$, uncorrected, cluster size <5.

Time-course analyses were conducted using a program written in MATLAB (MathWorks), as described previously (25). First, we created the ROI of the left somatosensory cortex, based on the electrophysiologically recorded point, using the Paxinos and Watson rat brain atlas (41) (Fig. 1*A*). Then, using the MATLAB program, we calculated the averaged signal values in the selected ROI. Percent changes in the BOLD, fMRI, or DfMRI signals were calculated as

$$\%\ \text{changes in signal intensity} = \left(\frac{\text{Averaged signals within ROI during activation period}}{\text{Averaged signals within ROI during baseline period}} - 1\right) \times 100,$$

where the basal period was 10 s before the stimulation in each block in electrical stimulation study. After the calculation, percent signal changes were averaged in five blocks. The averaged signal changes were then normalized for each rat. The FWHM was calculated as the time after which the signal decreased to 50% of the peak value.

In the hyperoxia study, we calculated the average signal changes in air, 100% O_2 replacement, and air replacement period.

The ADC was calculated for each condition (baseline, stimulation, hyperoxia challenge) as $ADC = \ln(S_{1,000}/S_{2,600})/1{,}600$, where $S_{1,000}$ and $S_{2,600}$ are the signal intensities (averaged over time for the baseline and hyperoxia conditions or at peak for the stimulation condition) obtained with b = 1,000 and 2,600 s/mm^2, respectively.

ACKNOWLEDGMENTS. We thank Olivier Reynaud and Nadya Pyatigorskaya for help with the initial experimental setup, Boucif Djemai for support with blood collection and general animal handling, Toshihiko Aso for advice on data handling, and Pierre Marquet for insightful comments regarding the manuscript.

1. Roy CS, Sherrington CS (1890) On the regulation of the blood-supply of the brain. *J Physiol* 11(1–2):85–158, 17.
2. Ogawa S, Lee TM, Kay AR, Tank DW (1990) Brain magnetic resonance imaging with contrast dependent on blood oxygenation. *Proc Natl Acad Sci USA* 87(24):9868–9872.
3. Logothetis NK, Pauls J, Augath M, Trinath T, Oeltermann A (2001) Neurophysiological investigation of the basis of the fMRI signal. *Nature* 412(6843):150–157.
4. Drake CT, Iadecola C (2007) The role of neuronal signaling in controlling cerebral blood flow. *Brain Lang* 102(2):141–152.
5. Nagaoka T, et al. (2006) Increases in oxygen consumption without cerebral blood volume change during visual stimulation under hypotension condition. *J Cereb Blood Flow Metab* 26(8):1043–1051.
6. Schachinger H, Klarhöfer M, Linder L, Drewe J, Scheffler K (2006) Angiotensin II decreases the renal MRI blood oxygenation level-dependent signal. *Hypertension* 47(6): 1062–1066.
7. Petridou N, et al. (2006) Direct magnetic resonance detection of neuronal electrical activity. *Proc Natl Acad Sci USA* 103(43):16015–16020.
8. Van der Linden A, et al. (2002) In vivo manganese-enhanced magnetic resonance imaging reveals connections and functional properties of the songbird vocal control system. *Neuroscience* 112(2):467–474.
9. Isokawa M (2005) N-methyl-D-aspartic acid-induced and Ca-dependent neuronal swelling and its retardation by brain-derived neurotrophic factor in the epileptic hippocampus. *Neuroscience* 131(4):801–812.
10. Holthoff K, Witte OW (1996) Intrinsic optical signals in rat neocortical slices measured with near-infrared dark-field microscopy reveal changes in extracellular space. *J Neurosci* 16(8):2740–2749.
11. Le Bihan D (2003) Looking into the functional architecture of the brain with diffusion MRI. *Nat Rev Neurosci* 4(6):469–480.
12. Darquié A, Poline JB, Poupon C, Saint-Jalmes H, Le Bihan D (2001) Transient decrease in water diffusion observed in human occipital cortex during visual stimulation. *Proc Natl Acad Sci USA* 98(16):9391–9395.
13. Le Bihan D, Urayama S, Aso T, Hanakawa T, Fukuyama H (2006) Direct and fast detection of neuronal activation in the human brain with diffusion MRI. *Proc Natl Acad Sci USA* 103(21):8263–8268.
14. Kohno S, et al. (2009) Water-diffusion slowdown in the human visual cortex on visual stimulation precedes vascular responses. *J Cereb Blood Flow Metab* 29(6):1197–1207.
15. Flint J, Hansen B, Vestergaard-Poulsen P, Blackband SJ (2009) Diffusion weighted magnetic resonance imaging of neuronal activity in the hippocampal slice model. *Neuroimage* 46(2):411–418.
16. Autio JA, et al. (2011) High b-value diffusion-weighted fMRI in a rat forepaw electrostimulation model at 7T. *Neuroimage* 57(1):140–148.
17. Miller KL, et al. (2007) Evidence for a vascular contribution to diffusion FMRI at high b value. *Proc Natl Acad Sci USA* 104(52):20967–20972.
18. Huttunen JK, et al. (2011) Evoked local field potentials can explain temporal variation in blood oxygenation level-dependent responses in rat somatosensory cortex. *NMR Biomed* 24(2):209–215.
19. Bosshard SC, et al. (2010) Assessment of brain responses to innocuous and noxious electrical forepaw stimulation in mice using BOLD fMRI. *Pain* 151(3):655–663.
20. Masamoto K, Vazquez A, Wang P, Kim SG (2008) Trial-by-trial relationship between neural activity, oxygen consumption, and blood flow responses. *Neuroimage* 40(2): 442–450.
21. Kim T, Masamoto K, Fukuda M, Vazquez A, Kim SG (2010) Frequency-dependent neural activity, CBF, and BOLD fMRI to somatosensory stimuli in isoflurane-anesthetized rats. *Neuroimage* 52(1):224–233.
22. Jensen NF, Todd MM, Kramer DJ, Leonard PA, Warner DS (1992) A comparison of the vasodilating effects of halothane and isoflurane on the isolated rabbit basilar artery with and without intact endothelium. *Anesthesiology* 76(4):624–634.
23. Jansson A, et al. (2004) Effects of isoflurane on prefrontal acetylcholine release and hypothalamic Fos response in young adult and aged rats. *Exp Neurol* 190(2):535–543.
24. Duong TQ (2007) Cerebral blood flow and BOLD fMRI responses to hypoxia in awake and anesthetized rats. *Brain Res* 1135(1):186–194.
25. Tsurugizawa T, Uematsu A, Uneyama H, Torii K (2010) Effects of isoflurane and alpha-chloralose anesthesia on BOLD fMRI responses to ingested L-glutamate in rats. *Neuroscience* 165(1):244–251.
26. Masamoto K, Fukuda M, Vazquez A, Kim SG (2009) Dose-dependent effect of isoflurane on neurovascular coupling in rat cerebral cortex. *Eur J Neurosci* 30(2):242–250.
27. Schulz K, et al. (2012) Simultaneous BOLD fMRI and fiber-optic calcium recording in rat neocortex. *Nat Methods* 9(6):597–602.
28. Franks NP (2008) General anaesthesia: From molecular targets to neuronal pathways of sleep and arousal. *Nat Rev Neurosci* 9(5):370–386.
29. Aso T, et al. (2009) An intrinsic diffusion response function for analyzing diffusion functional MRI time series. *Neuroimage* 47(4):1487–1495.
30. Stroman PW, Lee AS, Pitchers KK, Andrew RD (2008) Magnetic resonance imaging of neuronal and glial swelling as an indicator of function in cerebral tissue slices. *Magn Reson Med* 59(4):700–706.
31. Devor A, et al. (2003) Coupling of total hemoglobin concentration, oxygenation, and neural activity in rat somatosensory cortex. *Neuron* 39(2):353–359.
32. Hentschke H, Schwarz C, Antkowiak B (2005) Neocortex is the major target of sedative concentrations of volatile anaesthetics: Strong depression of firing rates and increase of GABAA receptor-mediated inhibition. *Eur J Neurosci* 21(1):93–102.
33. Lingamaneni R, Birch ML, Hemmings HC, Jr. (2001) Widespread inhibition of sodium channel-dependent glutamate release from isolated nerve terminals by isoflurane and propofol. *Anesthesiology* 95(6):1460–1466.
34. Ranft A, et al. (2004) Isoflurane modulates glutamatergic and GABAergic neurotransmission in the amygdala. *Eur J Neurosci* 20(5):1276–1280.
35. Schummers J, Yu H, Sur M (2008) Tuned responses of astrocytes and their influence on hemodynamic signals in the visual cortex. *Science* 320(5883):1638–1643.
36. Iadecola C (2004) Neurovascular regulation in the normal brain and in Alzheimer's disease. *Nat Rev Neurosci* 5(5):347–360.
37. Iadecola C, Nedergaard M (2007) Glial regulation of the cerebral microvasculature. *Nat Neurosci* 10(11):1369–1376.
38. Takagi S, Obata K, Tsubokawa H (2002) GABAergic input contributes to activity-dependent change in cell volume in the hippocampal CA1 region. *Neurosci Res* 44(3): 315–324.
39. Pannasch U, et al. (2011) Astroglial networks scale synaptic activity and plasticity. *Proc Natl Acad Sci USA* 108(20):8467–8472.
40. Le Bihan D (2007) The 'wet mind': Water and functional neuroimaging. *Phys Med Biol* 52(7):R57–R90.
41. Paxinos G, Watson C (1998) *The Rat Brain in Stereotaxic Coodinates* (Academic, San Diego), 4th Ed.